JOURNAL OF CATALYSIS 62, 35–43 (1980)

Carbon Deposition from Propylene on Polycrystalline and Single Crystal Iron

B. J. COOPER

SINTEF: Teknisk Kjemi, Norges Tekniske Høgskole, 7034 Trondheim-NTH, Norway

AND

D. L. TRIMM[1]

Institutt for Industriell Kjemi, Norges Tekniske Høgskole, 7034 Trondheim-NTH, Norway

Received June 26, 1978; revised September 4, 1979

The kinetics and morphology of the deposition of carbon from propylene on polycrystalline and single crystal iron have been studied over the temperature range 400–700°C. The dependence of the rate of carbon formation on temperature shows a pronounced maximum at ca. 600°C. Below this temperature, single crystals and polycrystalline iron foils behave similarly. On fresh samples, carbon deposition appears to be rate controlled by the diffusion of carbon in iron. After the deposition of some carbon it is suggested that the rate is controlled by the carbide-catalyzed production of carbon from propylene. Above ca. 600°C, carbon formation is considered to be rate controlled by the surface decomposition of propylene. On fresh samples, the rate was affected by the geometry of the surface with carbon formation decreasing in the order (100) ~ foils > (110). On used catalysts, where the active surface is probably iron carbide, geometric effects were not observed. Encapsulation of the surface by carbon was important at these higher temperatures, and this reaction was independent of the surface geometry.

INTRODUCTION

The deposition of carbon on transition metals is a matter of considerable interest in connection with the poisoning of catalysts. Attention has been focused mainly on unsupported and supported nickel, where a combination of kinetic and morphological observations has proved to be particularly useful in explaining the formation and gasification of carbon (*1–6*). At low temperatures (ca. 400–550°C) carbon formation is rate controlled by the diffusion of carbon through nickel, while between ca. 550 and 650°C the surface decomposition of hydrocarbons is rate determining. Gas phase production of carbon begins to be significant above about 650°C. These results have been found to be useful in explaining and minimizing carbon formation during reactions such as steam reforming (*1, 3*).

The system has been used to study the effect of surface geometry on catalytic reactions (*5*). As measured by the rate of deposition of carbon, the catalytic activity decreases in the order

$$(110) > (111) > (100).$$

In addition, surface roughness is found to affect carbon formation, since breakaway of nickel particles to give a higher catalytically active surface is easier on a rough surface.

Carbon deposition on other transition metals has not been studied to the same extent (*2, 4, 6–10*). There is evidence that the mechanism of the reaction may be the same (*8, 9*), since many common features are observed for deposition on iron, cobalt, and nickel. In at least one case, the mecha-

[1] To whom enquiries should be sent at the following present address: School of Chemical Technology, The University of New South Wales, Kensington 2033, N.S.W., Australia.

0021-9517/80/030035-09$02.00/0

nism of carbon formation may, however, be different (*11*). As a result of the renewed interest in iron as a Fischer–Tropsch catalyst (*12*), the present studies have been focused on the deposition of carbon on iron. Previous studies have suggested that the process is controlled by the rate of diffusion of carbon through iron (*10*). Whatever the cause, significant formation of carbon is known to occur and to result in catalyst deactivation.

The decomposition of carbon on iron from propylene has been used as a test reaction, and the problem has been approached using the techniques developed for the study of carbon formation on nickel (*1, 3*). Deposition on polycrystalline foils and on single crystals has been examined.

EXPERIMENTAL

Carbon deposition on iron was carried out in a flow system fitted with a C. I. Electronics Mk 2B balance. Propylene, hydrogen, and nitrogen were mixed and passed over the metal sample maintained at a preset temperature (±0.2°C): the weight uptake of the sample was measured continuously.

Polycrystalline iron foil (99.5% purity) was obtained from Goodfellow Metals and (100) and (110) orientation iron single crystals were obtained from Metals Research Ltd. Where necessary, samples were mechanically polished and electropolished. This was achieved using a series circuit, with the sample to be polished acting as the anode to an electrochemical cell containing a 50:50% mixutre of concn. HNO_3 and acetic anhydride maintained at 6°C. A current density of 1 A cm^{-3} was used, the anode–cathode distance being kept as small as possible. Samples were repeatedly electropolished until the surface was optically smooth: some deep pits in the foils could not be removed.

Carbon deposits were examined in the scanning electron microscope (SEM) and by electron probe microanalysis (EPMA).

RESULTS

Carbon deposition is known to be catalyzed by iron and by iron oxide (*14*). Preliminary studies showed that all oxide was reduced by heating in hydrogen at 700°C for at least 2 hr, and all samples were pretreated in this way.

Initial studies were focused on the effect of temperature. It was found necessary to add some hydrogen to the feed, since carbon formation ceased after a few minutes in its absence. At temperatures up to about 600°C, the rate of carbon deposition rapidly settled down to a constant value, but above this temperature the rate tended to fall away with time. Steady-state rates of carbon formation were plotted on a pseudo-Arrhenius graph (Fig. 1), from which comparisons of rate at the same temperature in an increasing or decreasing sequence gives some measure of the extent of deactivation. As with nickel (*1, 3*) a clearly distinguish-

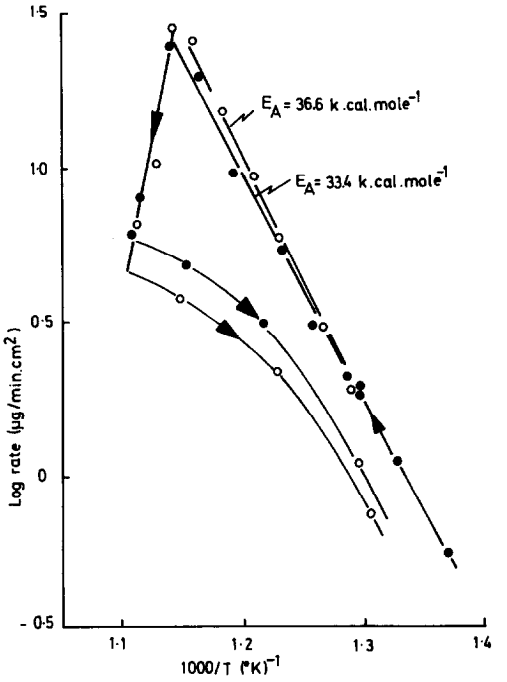

FIG. 1. Carbon deposition on foils as a function of temperature. Polycrystalline foil: 100 Torr C_3H_6; 100 Torr H_2. Prereduction in 20% H_2: N_2 for 2 hr at 700°C. ●, unpolished foil; ○, electropolished foil.

able temperature of maximum rate was observed (T_{max} = 500°C, nickel: T_{max} = 600°C, iron). Typical SEM pictures of deposits are shown in Fig. 2.

On the assumption that carbon deposition below and above T_{max} is controlled by different processes, studies of carbon formation were concentrated at 500 and 650°C. Deposition was followed on unpolished and electropolished polycrystalline iron foils

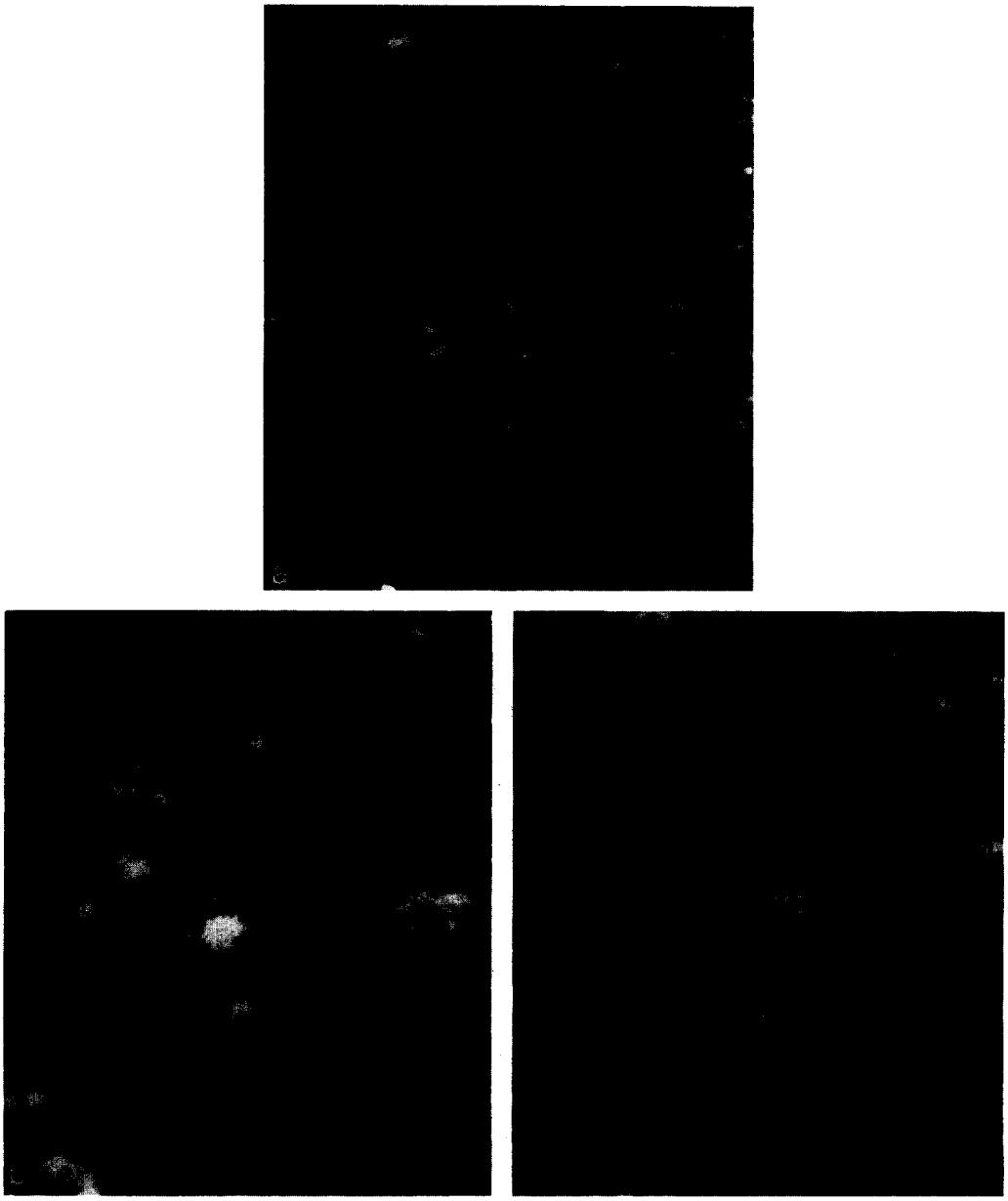

FIG. 2. Scanning electron micrographs of carbon deposits. (a) Reduction as per Fig. 1. Carbon deposited for 2 hr from 100 Torr C_3H_6; 100 torr H_2 at 500°C (total deposit 0.33 mg cm^{-2}) (×264). (b) Reduction as per Fig. 1. Carbon deposited for 2 hr as in (a) but at 570°C (total deposit 2 mg cm^{-2}) (×264). (c) Reduction as per Fig. 1. Carbon deposited for 2 hr as in (a) but at 665°C (total deposit 1.25 mg cm^{-2}) (×264).

and the results were compared with deposition on electropolished single crystals (Fig. 3). Each of these experiments was carried out using a fresh sample. Two effects are clearly seen. At both 500 and 650°C, electropolishing reduces carbon formation, an effect which extends over a range of temperature. At 500°C, carbon formation on all polished samples occurred at about the same rate but, at 650°C, carbon formation on the (110) single crystal was slower than on the other two samples. It was possible to carry out only two experiments with each single crystal, but the agreement (±4%) was such as to indicate that the difference was significant (see later). Homogeneous carbon formation was not significant at 650°C.

The effect of temperature on carbon formation on single crystals was then examined. In these experiments the same single crystal was used to measure the rates of carbon formation at different temperatures and the results are shown as a pseudo-Arrhenius plot in Fig. 4. For comparison, some similar experiments were carried out on polycrystalline foil (Fig. 5). These showed an unexpected effect in that the apparent activation energy at low temperatures decreased after carbon had been deposited on the foil. As a result, further studies were carried out in which carbon formation on used polycrystalline foils was compared with carbon formation on used single crystals (Fig. 6).

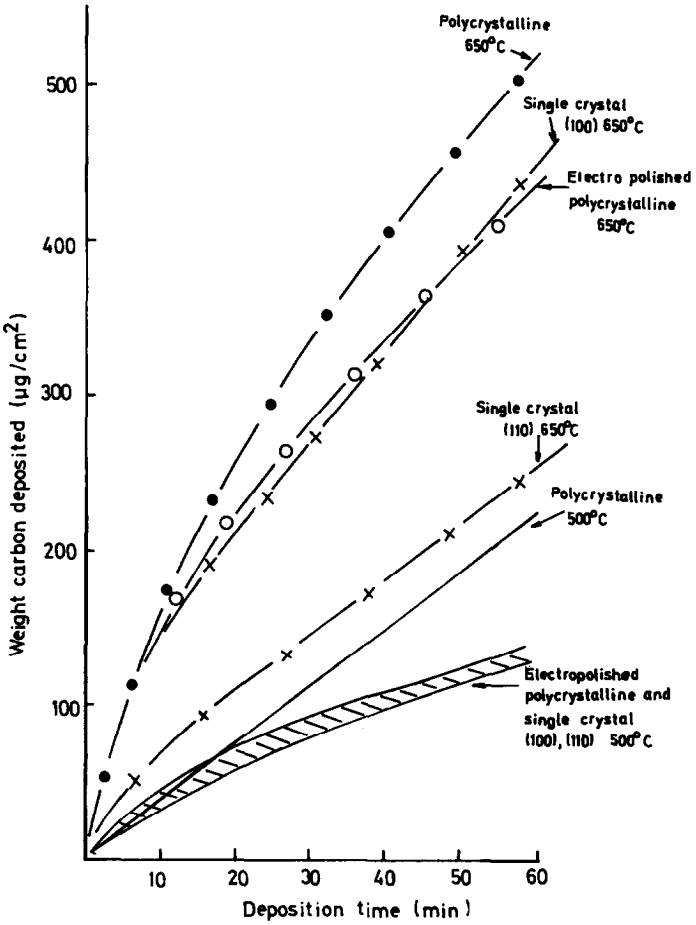

FIG. 3. Carbon production on different fresh iron samples: 100 Torr C_3H_6; 100 Torr H_2.

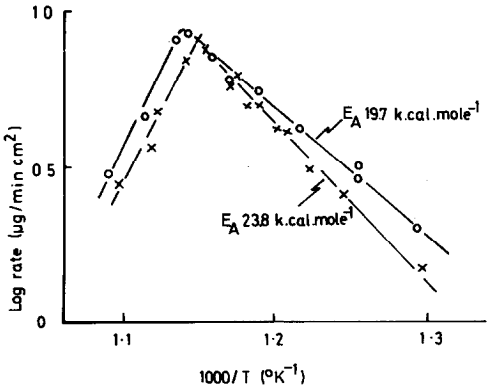

FIG. 4. Carbon formation on single crystals as a function of temperature: 100 Torr C_3H_6; 100 Torr H_2. O = (100) single crystal; × = (110) single crystal.

Attempts were made to measure orders of reaction in propylene and hydrogen but these were unsuccessful. The results tended to be irreproducible, although some general trends were noted. Thus, for example, carbon formation was always faster if the pressure of hydrogen was increased but appeared to be largely independent of the pressure of propylene.

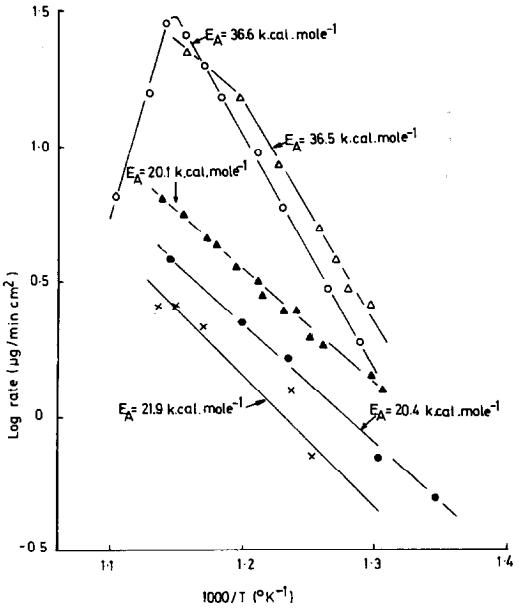

FIG. 5. Carbon deposition on new and used iron foils: effect of hydrogen: O, 100 Torr C_3H_6; 100 Torr H_2; new foil; △, 100 Torr C_3H_6; 200 Torr H_2; new foil; ●, 100 Torr C_3H_6; 100 Torr H_2; foil taken through one carbon formation temperature cycle (400–650°C), cooled, and used to obtain these results; ▲, 100 Torr C_3H_6; 200 Torr H_2; treated as above; ×, 100 Torr C_3H_6; Torr H_2; carbon deposited for 17 hr before being used to obtain these results.

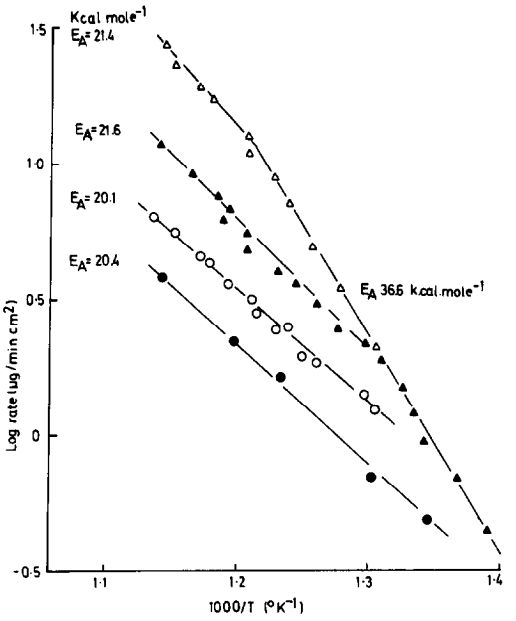

FIG. 6. Comparison of carbon deposition on used iron samples. All samples taken through a carbon formation temperature cycle (400–650°C) and then used to obtain these results: △, (100) single crystal: 100 Torr C_3H_6; 200 Torr H_2; ▲, (100) single crystal: 100 Torr H_3H_6; 100 Torr H_2; O, foil: 100 Torr C_3H_6; 200 Torr H_2; ●, foil: 100 Torr C_3H_2; 100 Torr H_2.

The possibility of gasification of carbon by hydrogen was then examined. Gasification was insignificant below 530°C but increased above this temperature. Gasification was found to be autocatalytic, presumably increasing as more iron particles are exposed (*1*). A steady rate was eventually achieved, and results pertinent to carbon formation studies are summarized in Fig. 7. The effect of gasification on the net rate of carbon formation is also shown on the same plot.

Examination of the deposit by EPMA showed that iron was always distributed throughout the carbon, presumably in the form of iron carbide (*10*). The concentration of iron was higher in deposits on polycrystalline foils than on single crystals, and the particles were ca. 50 μm in diameter.

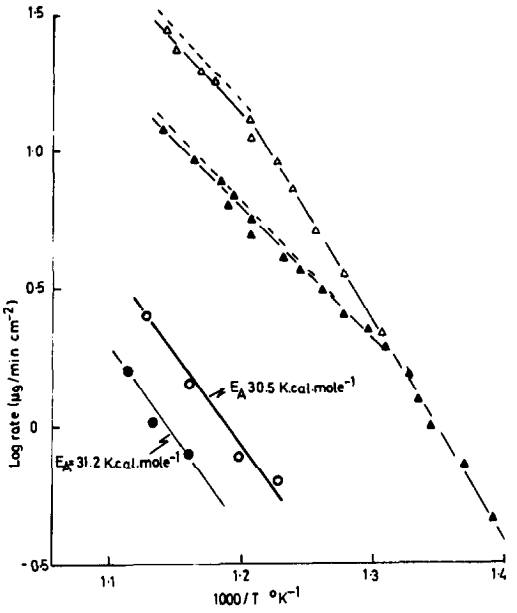

FIG. 7. Carbon deposition and gasification on (110) single crystal iron. Carbon deposition: △, 100 Torr C_3H_6; 200 Torr H_2; ▲, 100 Torr C_3H_6; 100 Torr H_2. Carbon gasification: ○, 200 Torr H_2; ●, 100 Torr H_2; ---, carbon deposition corrected for gasification.

DISCUSSION

Preliminary inspection of the results revealed that carbon formation on iron bears many similarities (and some differences) to carbon formation on nickel (*1, 3*). As a result, an analogous model for carbon formation was proposed which was found to be useful in explaining the result (Scheme 1).

The initial reactions (*1–3*) represent the adsorption and surface reactions of propylene to give monatomic carbon fragments. The evidence for monatomic fragments comes mainly from studies of C_2 molecules on iron. Anderson (*15*) has used molecular orbital calculations to show that ethylene and acetylene may be expected to dissociate into CH_2 and CH adsorbed fragments and that these should dehydrogenate on iron with a low activation energy. Similarly, Sinfelt (*16*) has suggested that the hydrogenolysis of ethane on iron is rate controlled by the hydrogenation–desorption kinetics of monocarbon fragments, and Dowie *et al.* (*17*) have shown that hydrogen–deuterium exchange during the hydrogenolysis of ethane, propane, and butane on iron leads to the monocarbon product CD_4.

Once formed, the fragments may react with hydrogen to give methane (reaction 4), may stay on the surface as an encapsulant (reaction 5), or may dissolve in the iron

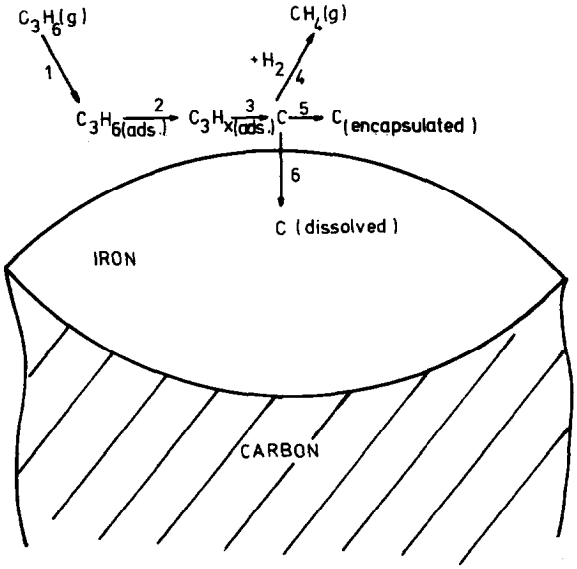

SCHEME 1. Diagramatic representation of proposed model of carbon formation on iron.

(reaction 6). By analogy with nickel (*1, 3*), this latter process would be expected to lead to migration of iron particles into the bulk carbon deposit.

Experimental observations tend to support this model. Methane was the only gaseous product to be identified and iron and carbon were found to migrate into each other. The decrease in the rate of carbon formation with time (Fig. 3) and the differences in carbon formation during temperature cycling (Fig. 1) are undoubtedly due to encapsulation.

The results were then examined to try to establish the rate-determining step. Considering first the findings for carbon formation at temperatures near to 500°C, a clear distinction could be made between carbon formation on fresh and used samples. Fresh samples of foils and single crystals behaved rather similarly. The reaction was approximately zero order in propylene but depended on hydrogen, and the apparent activation energy was ca. 36 ± 1 kcal mole ^{1} in all cases. (Figs. 1, 5, and 6). Used samples also behaved similarly although the results were different to those observed with fresh samples. The rate observed depended on the amount of carbon deposited (Figs. 1 and 5) and the apparent activation energy decreased to 21 ± 2 kcal mole^{-1} (Figs. 4 and 5).

An attempt was made to compare these results with published data for the iron–carbon system. Accepting the general model described in Scheme 1, the major process involves formation of monocarbon species on the surface, dissolution in and diffusion through the bulk iron, and precipitation of carbon from the iron. Gasification of monocarbon fragments, surface encapsulation by carbon, and the probable formation of iron carbides are complicating factors.

Possible mechanisms are summarized in Scheme 2, together with values reported for activation energies and heats of reaction of individual steps. The experimentally observed lack of dependence of rate on the pressure of propylene indicates that the formation of the original adsorbed species is not rate determining, and the similarity between the results for foils and for single crystals implies that grain boundaries are not important. Iron carbides are known to be produced (*10, 26–28*) and are worse catalysts for carbon formation than iron (*28, 29*).

Inspection of Scheme 2 in the light of the above showed that an explanation involving the intermediate formation of iron carbides explained all of the results observed. Monocarbon fragments are known to be able to diffuse on the surface to a nucleation center at or near the surface (*10*) where they are stabilized as iron carbide (*26*). This process continues until carbon is equilibrated between iron carbide and the underlying α-iron (*22*). If the rate-determining step is the migration of carbon from the iron carbide through the bulk α-iron, then the apparent activation energy should reflect the heat of solution of carbon in α-iron in equilibrium with iron carbide (17.3 kcal mole^{-1} (*22*)) and the activation energy of diffusion of carbon in α-iron (19.1 kcal mole^{-1} (*25*)). This gives a value of 36.4 kcal mole^{-1}, in good agreement with experimental values (ca. 36 kcal mole^{-1}).

As the deposition of carbon proceeds, encapsulation should build up and iron carbides will accumulate on the surface. These are worse catalysts for carbon formation than iron (*28, 29*), and a change in the rate-determining step can be expected. The change in the apparent activation energy to 21 ± 2 kcal mole^{-1} (Figs. 4 and 5) indicates that this occurs. Consideration of the model suggests that the new rate-determining step could well be the iron carbide catalyzed production of carbon from propylene, but this cannot be confirmed.

Although not proven, this explanation accounts for most of the experimental observations. It explains the migration of iron and carbon into each other, the preferential deposition at grain boundaries (Fig. 2), the difference in behavior of new and used

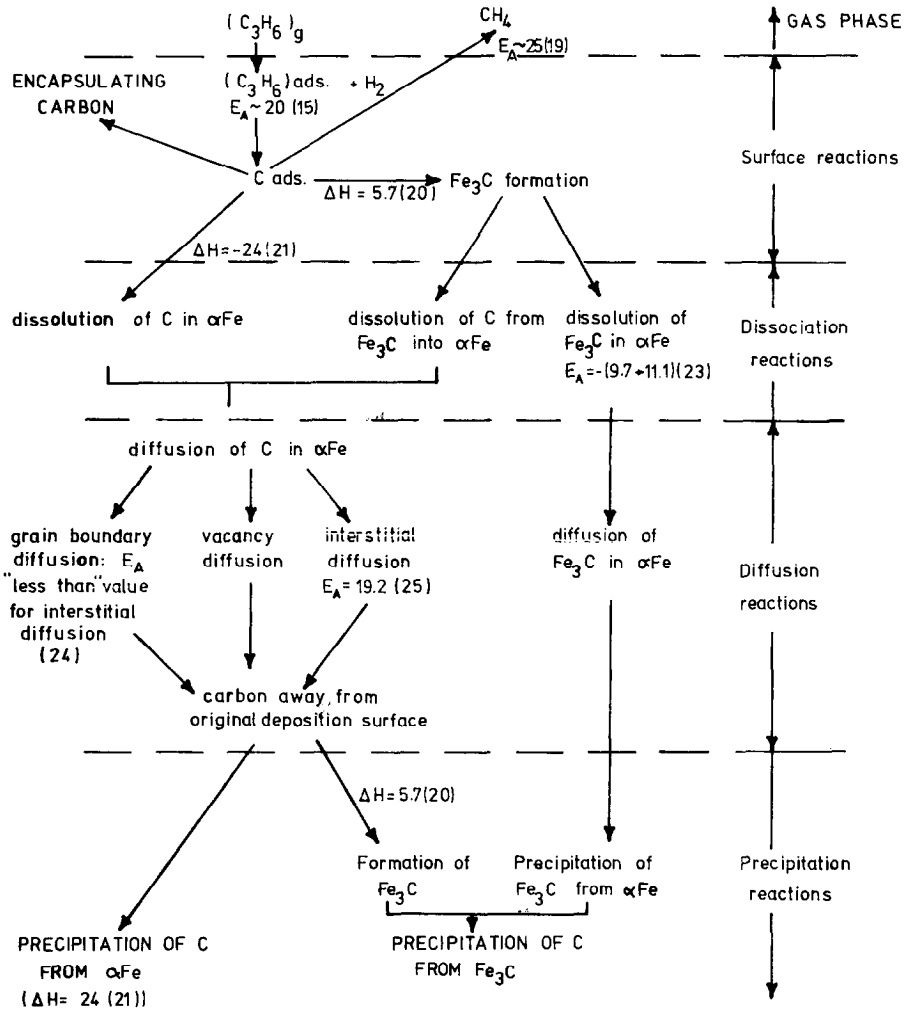

SCHEME 2. Migration of carbon through iron. Values are in kcal mole^{-1} with references in parentheses.

samples and, where this is possible, it accounts quantitatively for the observed values of activation energy. It also accounts for the fact that carbon formation is faster on unpolished samples (Fig. 3): breakaway of particles will be easier from rough surfaces, and this will lead to a higher concentration of iron in the carbon and, as a result, to faster carbon deposition.

Differences between fresh and used samples persisted at higher temperatures (around 650°C) although, in both cases, the apparent activation energy was negative (Figs. 1, 4, and 5). This is thought to be due to the fact that the surface reaction is rate controlling, when the apparent activation energy reflects the true activation energy and the heats of adsorption of reactants (*1, 3*)

$$E_{A_{app}} = E_{A_{app}} - \Delta H_{ads_{C_3H_6}} - \Delta H_{ads_{H_2}}.$$

As the temperature increases, the coverage of the surface by reactants will decrease, leading to a change of activation energy from positive to negative. This change will be exacerbated by the fact that a decrease in coverage of the surface by hydrogen will lead to enhanced encapsulation by carbon and, as a result, to a faster drop in the apparent activation energy.

On fresh samples (Fig. 3) there is clear evidence of a geometric effect on the rate of carbon formation, with the (100) face being more active than the (110) face. The similarity of the rate of carbon formation on foils to that on the (100) face is almost certainly due to the fact that the foil is predominantly (100) oriented (*30*). The existence of the geometric effect supports the suggestion that the surface reaction is rate controlling at these temperatures.

On the assumption that the decrease in rate with time (Fig. 3) is due to encapsulation, comparison of initial rates (no encapsulation) with rates after a given period of time should indicate the number of sites lost by encapsulation during that time. This decrease in rate was found to be the same for both the (100) and the (110) planes, indicating that encapsulation is structure insensitive.

On the used foils, this structure sensitivity disappears (Fig. 4). This is not surprising if the iron is converted to iron carbides, since the original crystal orientation would not be expected to be maintained.

The deposition of carbon on iron is seen to be even more complex than on nickel. The formation of encapsulating carbon occurs more readily and this will result in a higher loss of catalytic activity.

ACKNOWLEDGMENT

The authors wish to thank the Royal Norwegian Council for Scientific and Industrial Research for valuable financial support.

REFERENCES

1. Trimm, D. L., *Catal. Rev. Sci. Eng.* **16,** 155 (1977).
2. Baker, R. T. K., Barber, M., Harris, P., Feates, F. J., and Waite, R. J., *J. Catal.* **26,** 51 (1972).
3. Rostrup-Nielsen, J., and Trimm, D. L., *J. Catal.* **48,** 115 (1977).
4. Baker, R. T. K., Harris, P. S., Thomas, R. B., and Waite, R. J., *J. Catal.* **30,** 86 (1973).
5. Bernardo, C., and Trimm, D. L., *Carbon* **14,** 225 (1976).
6. Tamai, Y., Nishiyama, Y., and Takahashi, M., *Carbon* **7,** 209 (1969).
7. Robertson, S. D., *Carbon* **8,** 365 (1970); **10,** 221 (1972).
8. Baker, R. T. K., Feates, F. J., and Harris, P., *Carbon* **10,** 93 (1972).
9. Baker, R. T. K., Gadsby, G. R., and Terry, S., *Carbon* **13,** 245 (1975).
10. Oberlin, A., Endo, M., and Koyama, T., *J. Crystal Growth* **32,** 335 (1976).
11. Baker, R. T. K., and Waite, R. J., *J. Catal.* **37,** 101 (1975).
12. Madon, R. J., and Shaw, H., *Catal. Rev. Sci. Eng.* **15,** 69 (1977).
13. Rau, H., *J. Chem. Thermodynamics* **4,** 57 (1972).
14. Renshaw, G. D., Roscoe, C., and Walker, P. L., Jr., *J. Catal.* **18,** 164 (1970).
15. Anderson, A. B., *J. Amer. Chem. Soc.* **99,** 696 (1977).
16. Sinfelt, J. H., *Adv. Catal.* **23,** 91 (1973).
17. Dowie, R. S., Gray, M. C., Whan, D. A., and Kemball, C., *J. C. S. Chem. Commun.* 883 (1971).
18. Angus, H. T., "Cast Iron." Butterworths, London, 1976.
19. Sinfelt, J. H., and Yates, D. J. C., *J. Catal.* **10,** 362 (1968).
20. Perry, J. H., "Chemical Engineers Handbook," 4th Ed. McGraw-Hill, New York, 1969.
21. Swartz, J. C., *Trans. TMS-AIME* **245,** 1083 (1969).
22. Nolfi, F. V., Shewman, P. G., and Foster, J. S., *Met. Trans.* **1,** 2291 (1970).
23. Nolfi, F. V., Shewman, P. G., and Foster, J. S., *Met. Trans.* **1,** 789 (1970).
24. Gjostein, N. A., "Diffusion." American Society for Metals, Ohio, 1973.
25. Lord, A. E., and Beshers, D. N., *Trans. AIME* **239,** 680 (1967).
26. Krishtal, M. A., "Diffusion Process in Iron Alloys." Metallurgizdat, Moskva (1963); Israel Programme for Scientific Translation, Jerusalem (1970).
27. Fast, J. D., "Interaction of Metals and Gases," Vol. 2. Macmillan, New York, 1971.
28. Ruston, W. R., Warzee, M., Hennaut, J., and Waty, J., *Carbon* **7,** 47 (1969).
29. Eckstrom, H. C., and Adcock, W. A., *J. Amer. Chem. Soc.* **72,** 1042 (1950).
30. Taylor, A., "X-ray Metallography." Wiley, New York, 1961.
31. Morgan, D. W., and Kitchener, J. A., *Trans. Faraday Soc.* **50,** 51 (1954).